coatings

MDPI

Communication

SiO_2-Based Nanostructured Superhydrophobic Film with High Optical Transmittance

Algirdas Lazauskas [1,*], Dalius Jucius [1], Linas Puodžiukynas [2], Asta Guobienė [1] and Viktoras Grigaliūnas [1]

[1] Institute of Materials Science, Kaunas University of Technology, K. Baršausko 59, LT51423 Kaunas, Lithuania; dalius.jucius@ktu.lt (D.J.); asta.guobiene@ktu.lt (A.G.); viktoras.grigaliunas@ktu.lt (V.G.)

[2] Department of Physics, Kaunas University of Technology, Studentu St. 50, LT51368 Kaunas, Lithuania; linas.puodziukynas@ktu.lt

* Correspondence: algirdas.lazauskas@ktu.edu; Tel.: +370-671-73375

Received: 26 August 2020; Accepted: 28 September 2020; Published: 29 September 2020

Abstract: Superhydrophobic and transparent films would be very useful in optoelectronic applications where non-wetting is desired. Herein, hexamethyldisilazane was used for functionalization of fumed SiO_2 nanoparticles via silylation derivatization reaction. Modified fumed SiO_2 nanoparticle dispersion was used for fabrication of SiO_2-based nanostructured film via drop-casting method. This film exhibited a combination of high optical transmittance in the visible spectrum portion and superhydrophobicity (163° ± 1° and hysteresis as low as ~2°). This was possible to achieve due to the submicrometer-scale roughness (R_q = 252.7 nm) and branched network structure of the film surface with convenient surface chemistry of hydrophobic methyl groups. The method reported herein is not complicated, allows for obtaining large quantities of modified SiO_2 nanoparticle dispersions and can be used in combination with other deposition methods.

Keywords: SiO_2; nanostructured; functional; superhydrophobic; film; transparent

1. Introduction

Multifunctional superhydrophobic coatings and films having several functional properties are gaining increased attention with continued demand for widespread applications in both applied science and industry. Specifically, a substantial scientific interest is to enhance the optical transmittance of the superhydrophobic coatings or films in order to efficiently integrate them in optoelectronic applications e.g., solar cells, phone screens, wearable electronics, smart windows etc. However, a combination of high optical transmittance in the visible spectrum portion and superhydrophobicity is a real challenge to achieve as the latter requires sufficient surface roughness present, which, unfortunately, leads to extensive scattering of propagated light.

A number of works have been devoted to the fabrication of transparent superhydrophobic coatings and films. Silane-based microporous and transparent superhydrophobic film with a water contact angle (CA) of 164° was deposited via sol-gel technique in [1]. SiO_2/poly(dimethylsiloxane) composite coatings [2] exhibited high optical transmittance and superhydrophobicity (CA 158°). High optical transmittance as well as superoleophobicity was obtained using spray deposition of sol-gel-fluorinated submicrometer-sized fumed SiO_2 particles (also known as amorphous SiO_2) [3]. A superhydrophobic and partially transparent coating with a CA > 164° was developed using the hierarchical surface roughness of methylsilane particles [4]. An advanced chemical vapor deposition technique [5] was employed for deposition of superhydrophobic SiO_2 coatings, which demonstrated high optical transmittance in the visible spectrum portion with a CA of 165°. Transparent polyurethane and a fumed SiO_2 coating with superhydrophobic and self-cleaning behavior were deposited via spray

technique in [6]. A novel advanced spray-based layer-by-layer coating technique was developed in [7], where a highly transparent superhydrophobic coating (CA > 173°) had a layered structure consisting of SiO_2 nanoparticles and different organosilane compounds. In [8], a suspension of SiO_2 microspheres and poly(dimethylsiloxane) was used for fabrication of a highly transparent, superhydrophobic and self-cleaning coating. A two-layer combination was applied in [9], where adhesive and hydrophobic suspensions of SiO_2 nanoparticles (average size 16 nm) were sprayed in succession on various surfaces leading to a CA of about 160°. In most cases, for the combination of high optical transmittance and superhydrophobicity to work, surface roughness should be adjusted to submicrometer scale.

In this work, a SiO_2-based nanostructured superhydrophobic film was fabricated using a simple drop-casting deposition method. The alkyl-functional silane was used to modify fumed SiO_2 nanoparticles by substitution of hydrogen in hydroxyl groups with trimethylsilyl group via silylation derivatization reaction. Specifically, hexamethyldisilazane (HMDS) was used as a silylating agent due to its high availability in semiconductor purity [10]. Furthermore, this approach can be used for the preparation of large quantities of modified SiO_2 nanoparticle dispersions in combination with other thin film fabrication methods, e.g., dip-coating, spray-coating, spin-coating and Langmuir-Blodgett deposition. Importantly, the fabricated SiO_2-based nanostructured film exhibited a combination of high optical transmittance in the visible spectrum portion and superhydrophobicity.

2. Materials and Methods

2.1. Materials

HMDS of analytical grade (≥99%, Sigma-Aldrich, Saint Louis, MO, USA), ethanol (96%, MV Group Production, Kaunas, Lithuania) and fumed SiO_2 (CAS 112945-52-5, Sigma-Aldrich, Saint Louis, MO, USA) were used as received. The surface area of thr fumed SiO_2 was specified to be 175–225 m^2/g. Ultrapure water with a resistivity higher than 18.2 MΩ/cm at 25 °C was used in all experiments, and was obtained from a Direct-Q® 3 UV water purification system (Merck KGaA, Darmstadt, Germany). Microscope glass slides HistoBond®+ were obtained from Paul Marienfeld GmbH & Co. KG (Lauda-Königshofen, Germany).

2.2. Fabrication of SiO_2-Based Nanostructured Superhydrophobic Surface

The silylation derivatization reaction of fumed SiO_2 with HDMS was performed for 3 h at 210 °C. The amount of silylating agent was 20% of the fumed SiO_2 weight. The fumed SiO_2 was loaded into a glass reactor with a stirrer. Afterwards, all air was purged from the reactor with N_2 gas, followed by heating to the desired temperature. The HDMS was added to the reactor through the spray inlet valve. After completion of the process, the appropriate amount of fumed SiO_2 was added to the glass flask containing ethanol and sonicated for 30 min. Then, the dispersion was left undisturbed for 3 h in order to settle out large fumed SiO_2 fragments. The resultant modified fumed SiO_2 nanoparticle dispersion was drop-casted on the microscope glass slides and ethanol was removed by evaporation at room temperature. The 0.5 mL of the modified fumed SiO_2 nanoparticle dispersion was sufficient to produce a uniform film on the microscope glass slide.

2.3. Characterization

Atomic force microscopy (AFM) experiments were carried out at room temperature using a NanoWizardIII atomic force microscope (JPK Instruments, Bruker Nano GmbH, Berlin, Germany), while the data were analyzed using a SurfaceXplorer and JPKSPM Data Processing software (Version spm-4.3.13, JPK Instruments, Bruker Nano GmbH). The AFM images were collected using a V-shaped silicon cantilever (spring constant of 3 N/m, tip curvature radius of 10.0 nm and the cone angle of 20°) operating in contact mode. For supportive surface imagining, a Raith e-LiNEplus scanning electron microscope (SEM, Dortmund, Germany) was used. CA measurements were performed at room temperature using the sessile drop method. A droplet of deionized water (5 μL) was deposited

onto the investigated surface. Optical images of the droplet were recorded with a PC-connected digital camera after 10 s of dropping and CA measurements were carried out using an active contour method based on B-spline snakes (active contours) [11]. The contact angle hysteresis was measured as the difference between the advancing and receding contact angle of a sliding droplet. Sliding angle was measured as the point at which hysteresis force was no longer capable of resisting the water droplet from moving. An optical spectrometer, Avantes, that is composed of a deuterium halogen light source (AvaLight DHc, Avantes, Apeldoorn, The Netherlands), and a spectrometer (Avaspec-2048, Avantes, Apeldoorn, The Netherlands) were used to record UV-visible light absorbance spectra. Raman spectra were recorded using an inVia Raman spectrometer (Renishaw, Wotton-under-Edge, UK) equipped with a CCD camera and confocal microscope (50× objective). The Raman spectra were excited with 532 nm radiation of semiconductor green laser. The 2400 lines/mm grating was used to record the Raman spectra.

3. Results and Discussion

AFM analysis of SiO_2-based nanostructured film (Figure 1a) was conducted over the considerably large 20 × 20 μm^2 area for quantitative morphological evaluation. In contrast to the nominal area of the topographical image, the full area was found to be 705.653 nm^2, as measured by AFM. The topography of the film surface exhibits a random distribution of surface features having different angle orientations to each other, without a preferred direction. A mean height of the surface structures (Z_{mean}) was determined to be 402.6 nm. The root mean square roughness (R_q) was found to be 252.7 nm. The surface has a nearly symmetrical height distribution (i.e., as many peaks as valleys) with a skewness (R_{sk}) value approaching zero and exhibits a platykurtoic distribution of the morphological features with a kurtosis (R_{ku}) value of 1.81.

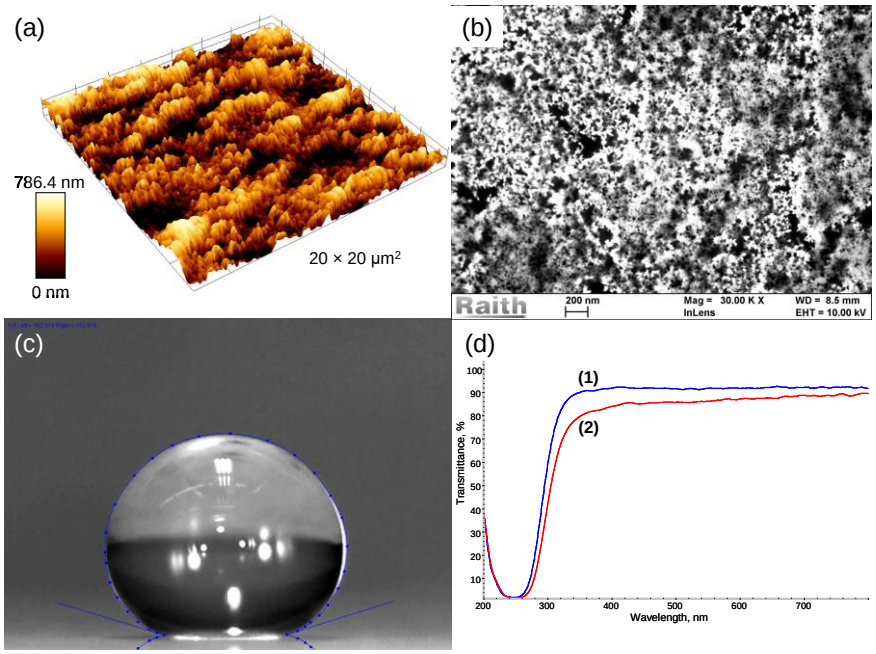

Figure 1. Atomic force microscopy (AFM) 3D surface topography (**a**), SEM micrograph (**b**) and water droplet profile image (**c**) of the SiO_2-based nanostructured film. UV-visible transmission spectra (**d**) of bare glass (1) and corresponding modified fumed SiO_2-coated glass (2).

A higher magnification SEM micrograph (Figure 1b) of the film surface revealed that it is assembled of quasi-spherical nanoparticles of sizes in the range of ~10–35 nm. It can be seen from SEM micrograph that nanoparticles are assembled in the form of a branched network structure, with plenty of space left for air pocket inclusions, indicating that it is not a close-packing nanoparticle assembly [12,13], and

Cassie-Baxter-like composite wetting mode is characteristic for this type of surface [14]. Figure 1c shows the water droplet profile on the corresponding SiO_2-based nanostructured film surface. The static CA was determined to be 163° ± 1°, which effectively exhibits superhydrophobic characteristics. The CA hysteresis and sliding angle were determined to be ~2° and ~4°, respectively, supporting SEM observations. The UV-visible transmission spectra of bare and modified fumed SiO_2-coated microscope glass slides are shown in Figure 1d. The transmittance of wavelengths in the range of 380–800 nm decreases by only a small percentage for modified fumed SiO_2-coated microscope glass slides as compared to the bare ones, thus the coating can be considered highly transparent in the visible spectrum portion. This result also supports the AFM analysis, that surface roughness should be at a submicrometer scale in order to achieve the combination of high optical transmittance and superhydrophobicity, in agreement with previous studies reviewed in the Introduction section. The synergistic effect of convenient surface morphology and chemistry is mainly responsible for this combination (Video S1) working.

The self-cleaning performance of the SiO_2-based nanostructured film (Figure 2) was investigated using candle soot powder as the target contaminant. The modified fumed SiO_2-coated glass was tilted at ~30° and the contaminant powder was randomly sprinkled on the surface of the film. Afterwards, water droplets were poured on the surface of the superhydrophobic film. It can be clearly seen in Video S2 that when the water droplets impacted the surface of superhydrophobic film, they bounced and then rolled off, taking contaminant away and, at the same time, leaving a clean path track behind them. This result shows the excellent self-cleaning performance of the SiO_2-based nanostructured film. The observed water droplet bouncing behavior is also an indication of outstanding superhydrophobic characteristics of the fabricated film, in line with [15].

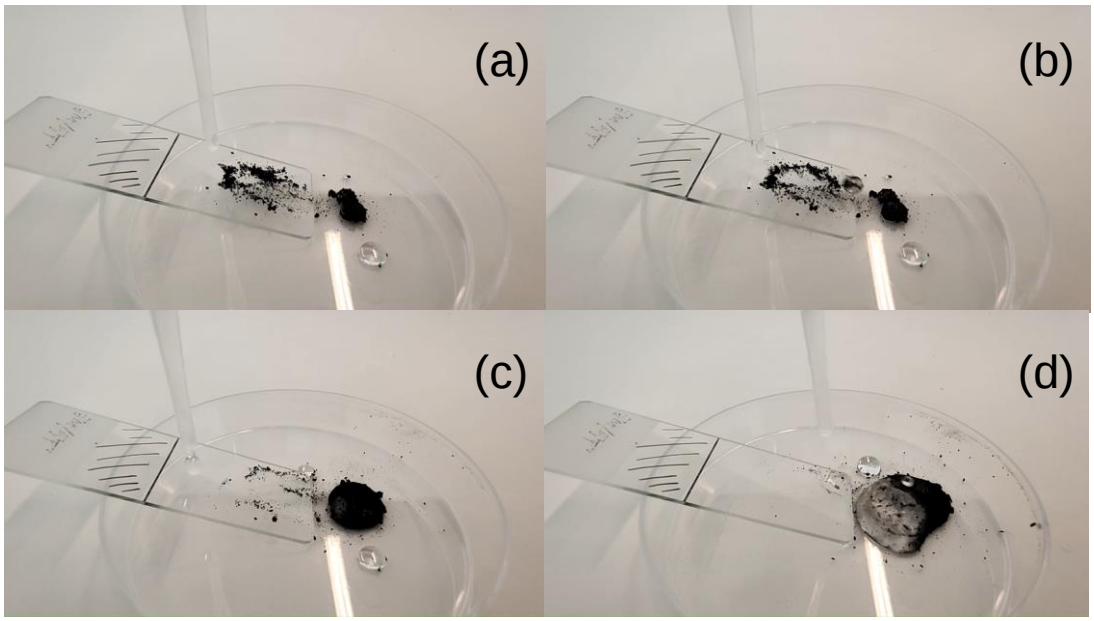

Figure 2. Self-cleaning process on the modified fumed SiO_2 coated glass: the surface with candle soot powder as the target contaminant (**a**), the surface with water droplets on it (**b**,**c**) and the surface after the process (**d**).

Figure 3a shows Raman spectrum of modified fumed SiO_2-coated glass. Low-frequency range (<1200 cm^{-1}) of the Raman spectrum contains the bands typical for the siloxane bonds. The band at 139 cm^{-1} can be attributed to the boson peak of the SiO_2 network [16]. The bands at 450 and 559 cm^{-1} correspond to Si–O–Si symmetric stretching of Q4 and Q3 species, respectively. The band at 780 cm^{-1} should be attributed to Si motions in its tetrahedral oxygen cage, whereas the 957 and 1094 cm^{-1} bands correspond to Si–O stretching vibration modes of Q2 and Q3 species, respectively [17,18].

Above 1400 cm^{-1}, the Raman spectrum contains a number of peaks characteristic to vibrational modes of hydrophobic methyl groups, thus confirming that fumed SiO_2 was successfully modified via silylation derivatization reaction. The bands at 1418 and 1443 cm^{-1} can be associated to the deformation of $–CH_3$ group, while the bands at 2849–3015 cm^{-1} can be associated to the symmetric and asymmetric stretches of $–CH_3$ groups [19–21]. For reference purposes, vibrational modes of methyl groups are not present in Raman spectrum of bare fumed SiO_2-coated glass (Figure 3b). Raman bands at the range of 1500–2800 cm^{-1} arise due to the combination modes and overtones of the silica matrix [22].

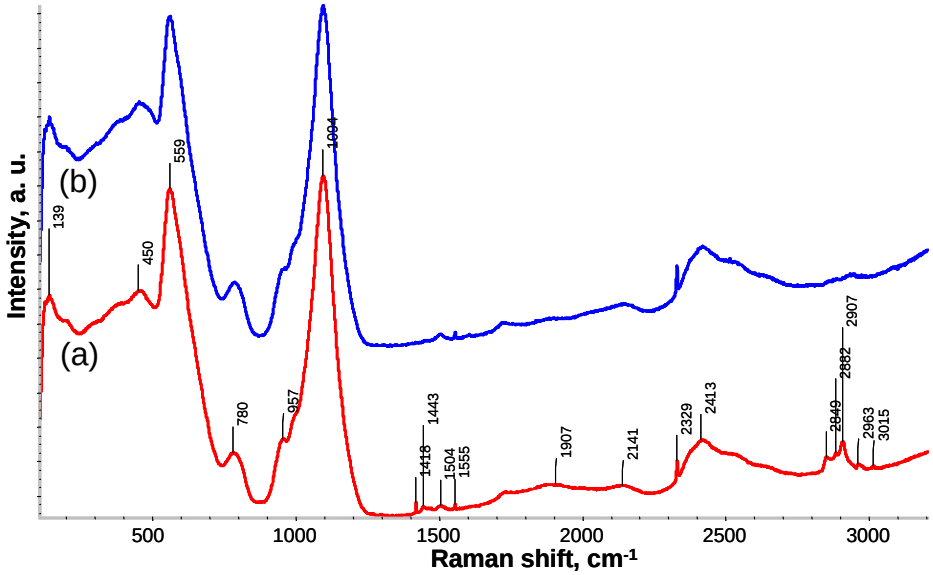

Figure 3. Raman spectrum of modified (**a**) and bare (**b**) fumed SiO_2-coated glass.

The mechanical durability of SiO_2-based nanostructured film was investigated employing sand abrasion tests [23]. The typical test in progress is demonstrated in Video S3. Sand grains with a diameter in the range of 50–200 μm were used in the sand abrasion tests. The modified fumed SiO_2 film surface retained its superhydrophobic properties for 6 s of sand abrasion from a height of 5 cm with a CA of 152° ± 1°. Further increase in sand impact height or test time resulted in the loss of superhydrophobicity.

To summarize, we have designed a novel and uncomplicated approach for fabrication of superhydrophobic, self-cleaning and highly transparent film. It can be used in many different optoelectronic applications where extensive mechanical contact with other surfaces is not required. For instance, precision optical glass scales and reticles are used in analytical instrumentation, motion control and other optics markets. The precision of these optical components is also highly dependent on the cleanliness of the surface. SiO_2-based nanostructured film can be used as protective layer against dust particles and other contaminants while, at the same time, ensuring high optical transmittance in the wavelength range of 380–800 nm.

4. Conclusions

HDMS was used for functionalization of fumed SiO_2 nanoparticles by substitution of hydrogen in hydroxyl groups with trimethylsilyl group via silylation derivatization reaction. A simple drop-casting method was employed for deposition of thin film from modified fumed SiO_2 nanoparticle dispersion. The surface morphology and wetting, optical and chemical properties of SiO_2-based nanostructured film were investigated. The following conclusions were drawn:

(1) The film surface exhibited a branched network structure composed of interconnected quasi-spherical nanoparticles (size ~10–35 nm) with submicrometer-scale roughness (R_q = 252.7 nm).

(2) The fabricated film exhibited a composite wetting mode and was found to be effectively superhydrophobic with CA of 163 ± 1° and hysteresis as low as ~2°, which was attributed to the synergistic effect of convenient surface morphology and chemistry.
(3) The superhydrophobic film exhibited an excellent self-cleaning performance.
(4) The SiO_2-based nanostructured film exhibited high optical transmittance in the visible spectrum portion. This was possible to achieve due to the submicrometer-scale roughness and branched network structure of the film surface.
(5) Raman analysis determined a number of vibrational modes corresponding to hydrophobic methyl groups, thus confirming that fumed SiO_2 was successfully modified via silylation derivatization reaction.
(6) The method presented herein is not complicated, allows for obtaining large quantities of modified SiO_2 nanoparticle dispersions and can be used in combination with dip-coating, spray-coating, spin-coating, drop-casting and Langmuir-Blodgett deposition.

Supplementary Materials: The following are available online at http://www.mdpi.com/2079-6412/10/10/934/s1, Video S1: video illustration of high optical transmittance and superhydrophobicity in action—fabricated SiO_2-based nanostructured film on glass substrate; Video S2: self-cleaning performance of the SiO_2-based nanostructured film on glass substrate. Candle soot powder is used as a target contaminant. Video is captured in slow motion using camera shoots of 240 frames per second. Video S3: typical sand abrasion test in progress. Video is captured in slow motion using camera shoots of 240 frames per second.

Author Contributions: Conceptualization, A.L.; Methodology, A.L., V.G., and D.J.; Validation, A.L., L.P., and D.J.; Formal analysis, A.L., V.G., and D.J.; Investigation, A.L., A.G., D.J. and L.P.; Resources, A.L.; Writing—original draft preparation, A.L., V.G., and D.J.; Writing—review and editing, A.L., V.G. and D.J.; Visualization, A.L., V.G., and D.J.; Supervision, A.L.; Project administration, A.L.; Funding acquisition, A.L. All authors have read and agreed to the published version of the manuscript.

Funding: This research was funded by the European Social Fund under the No. 09.3.3-LMT-K-712-01 "Improvement of researchers' qualification by implementing world-class R&D projects" measure. Grant No. 09.3.3-LMT-K-712-01-0074.

Acknowledgments: A special thanks goes to project members Valentinas Baltrušaitis, Rimantas Gudaitis, Brigita Abakevičienė, Igoris Prosyčevas, Mindaugas Andrulevičius and Simas Račkauskas from Kaunas University of Technology for their technical assistance.

Conflicts of Interest: The authors declare no conflict of interest.

References

1. Li, W.; Liang, Z.; Dong, B.; Tang, H. Transmittance and self-cleaning polymethylsiloxane coating with superhydrophobic surfaces. *Surf. Eng.* **2019**, *36*, 574–582. [CrossRef]
2. Liang, Z.; Geng, M.; Dong, B.; Zhao, L.; Wang, S. Transparent and robust SiO_2/PDMS composite coatings with self-cleaning. *Surf. Eng.* **2019**, *36*, 643–650. [CrossRef]
3. Yang, J.; Li, J.; Xu, P.; Chen, B. Robust and transparent superoleophobic coatings from one-step spraying of SiO_2@ fluoroPOS. *J. Sol-Gel Sci. Technol.* **2020**, *93*, 79–90. [CrossRef]
4. Ardekani, S.R.; Aghdam, A.S.R.; Nazari, M.; Bayat, A.; Saievar-Iranizad, E. A new approach for preparation of semi-transparent superhydrophobic coatings by ultrasonic spray hydrolysis of methyltrimethoxysilane. *Prog. Org. Coat.* **2019**, *135*, 248–254. [CrossRef]
5. Tombesi, A.; Li, S.; Sathasivam, S.; Page, K.; Heale, F.L.; Pettinari, C.; Carmalt, C.J.; Parkin, I.P. Aerosol-assisted chemical vapour deposition of transparent superhydrophobic film by using mixed functional alkoxysilanes. *Sci. Rep.* **2019**, *9*, 7549. [CrossRef]
6. Wang, Q.; Chen, G.; Tian, J.; Yu, Z.; Deng, Q.; Yu, M. Facile fabrication of fluorine-free, transparent and self-cleaning superhydrophobic coatings based on biopolymer castor oil. *Mater. Lett.* **2018**, *230*, 84–87. [CrossRef]
7. Siri, R.; Thongrom, S.; van Dommelen, P.; Muensit, N.; Daengngam, C. Demonstrating spray deposition of self-regulated nanorough layers for stable transparent superhydrophobic film coatings. *Thin Solid Films* **2019**, *686*, 137429. [CrossRef]

8. Su, Q.; Wen, F.; Huang, Y.; Wang, B. Abrasion resistant semitransparent self-cleaning coatings based on porous silica microspheres and polydimethylsiloxane. *Ceram. Int.* **2019**, *45*, 401–408. [CrossRef]
9. Chen, C.; Weng, D.; Chen, S.; Mahmood, A.; Wang, J. Development of Durable, Fluorine-free, and Transparent Superhydrophobic Surfaces for Oil/Water Separation. *ACS Omega* **2019**, *4*, 6947–6954. [CrossRef] [PubMed]
10. Smith, B.W.; Suzuki, K. *Microlithography: Science and Technology*; CRC Press: Boca Raton, FL, USA, 2018; p. 662.
11. Stalder, A.F.; Kulik, G.; Sage, D.; Barbieri, L.; Hoffmann, P. A snake-based approach to accurate determination of both contact points and contact angles. *Colloids Surf. A Physicochem. Eng. Asp.* **2006**, *286*, 92–103. [CrossRef]
12. Genzer, J.; Efimenko, K. Creating long-lived superhydrophobic polymer surfaces through mechanically assembled monolayers. *Science* **2000**, *290*, 2130–2133. [CrossRef] [PubMed]
13. Genzer, J.; Efimenko, K. Recent developments in superhydrophobic surfaces and their relevance to marine fouling: A review. *Biofouling* **2006**, *22*, 339–360. [CrossRef] [PubMed]
14. Parvate, S.; Dixit, P.; Chattopadhyay, S. Superhydrophobic Surfaces: Insights from Theory and Experiment. *J. Phys. Chem. B* **2020**, *124*, 1323–1360. [CrossRef] [PubMed]
15. Crick, C.R.; Parkin, I.P. Water droplet bouncing—A definition for superhydrophobic surfaces. *Chem. Commun.* **2011**, *47*, 12059–12061. [CrossRef]
16. Kacem, I.B.; Gautron, L.; Coillot, D.; Neuville, D.R. Structure and properties of lead silicate glasses and melts. *Chem. Geol.* **2017**, *461*, 104–114. [CrossRef]
17. Nekvindova, P.; Svecova, B.; Stanek, S.; Vytykacova, S.; Mackova, A.; Malinsky, P.; Machovic, V.; Spirkova, J. The Raman spectroscopy use for monitoring of changes in the glass structure of the thin layers caused by ion implantation. *Ceram. Silikáty* **2015**, *59*, 187–193.
18. Deschamps, T.; Martinet, C.; Bruneel, J.; Champagnon, B. Soda-lime silicate glass under hydrostatic pressure and indentation: A micro-Raman study. *J. Phys. Condens. Matter* **2011**, *23*, 035402. [CrossRef]
19. Volovšek, V.; Furić, K.; Bistričić, L.; Leskovac, M. *Micro Raman Spectroscopy of Silica Nanoparticles Treated with Aminopropylsilanetriol*; Macromolecular symposia, Wiley Online Library: Weinheim, Germany, 2008; pp. 178–182.
20. Schneider, B.; Štokr, J.; Schmidt, P.; Mihailov, M.; Dirlikov, S.; Peeva, N. Stretching and deformation vibrations of CH2, C (CH3) and O (CH3) groups of poly (methyl methacrylate). *Polymer* **1979**, *20*, 705–712. [CrossRef]
21. Song, Y.; Huang, Y.; Havenga, E.A.; Butler, I.S. Vibrational spectra of crystalline tetrakis (trimethylsilyl) silane (IV), Si [Si (CH3) 3] 4, at high pressures. *Vib. Spectrosc.* **2001**, *27*, 127–134. [CrossRef]
22. Efimov, A.M.; Pogareva, V.G. IR absorption spectra of vitreous silica and silicate glasses: The nature of bands in the 1300 to 5000 cm−1 region. *Chem. Geol.* **2006**, *229*, 198–217. [CrossRef]
23. Deng, X.; Mammen, L.; Butt, H.-J.; Vollmer, D. Candle soot as a template for a transparent robust superamphiphobic coating. *Science* **2012**, *335*, 67–70. [CrossRef] [PubMed]

© 2020 by the authors. Licensee MDPI, Basel, Switzerland. This article is an open access article distributed under the terms and conditions of the Creative Commons Attribution (CC BY) license (http://creativecommons.org/licenses/by/4.0/).